Inorganic Chemistry
Article

Inorg. Chem. **2010**, *49*, 6889–6896 **6889**
DOI: 10.1021/ic100339f

Core Conversion Reactions of the Cubane-Type Metal-Sulfido Clusters: Shape Shift, Contraction, and Expansion of the MM′Re_2S_4 Cubanes (M = Ir, Rh, Ru; M′ = Pt, Pd)

Rie Shibata, Hidetake Seino, Shunpei Fujii, and Yasushi Mizobe*

Institute of Industrial Science, The University of Tokyo, Komaba, Meguro-ku, Tokyo 153-8505, Japan

Received February 22, 2010

Treatment of incomplete cubane-type clusters $[(Cp^*M)\{Re(L)\}_2(\mu_3\text{-}S)(\mu_2\text{-}S)_3]$ (M = Ir (**1a**), Rh (**1b**); Cp* = η^5-C_5Me_5; L = $S_2C_2(SiMe_3)_2$) and $[\{(Pmb)Ru\}\{Re(L)\}_2(\mu_3\text{-}S)(\mu_2\text{-}S)_3]$ (Pmb = η^6-C_6Me_5H) with 1 equiv of $[Pt(PPh_3)_3]$ gave tetranuclear tetra(sulfido) clusters having raft-type cores, $[(Cp^*M)\{Pt(PPh_3)_2\}\{Re(L)\}_2(\mu_3\text{-}S)_4]$ (M = Ir (**3a**), Rh) and $[\{(Pmb)Ru\}\{Pt(PPh_3)_2\}\{Re(L)\}_2(\mu_3\text{-}S)_4]$, which presents a sharp contrast to the reactions with $[Pd(PPh_3)_4]$ reported previously, affording the cubane-type clusters $[(Cp^*M)\{Pd(PPh_3)\}\{Re(L)\}_2(\mu_3\text{-}S)_4]$ (M = Ir (**2a**), Rh) and $[\{(Pmb)Ru\}\{Pd(PPh_3)\}\{Re(L)\}_2(\mu_3\text{-}S)_4]$. The reactions of **2a** with diphosphines **P2** resulted in the conversion of its cubane-type core into the analogous raft-type frameworks, forming $[(Cp^*Ir)\{Pd(\mathbf{P2})\}\{Re(L)\}_2(\mu_3\text{-}S)_4]$ (**P2** = *cis*-$Ph_2PCH{=}CHPPh_2$ (**6**), $Ph_2PCH_2CH_2PPh_2$, $Ph_2PCH_2CH_2CH_2PPh_2$). On the other hand, when **2** was allowed to react with $Ph_2PCH_2PPh_2$ (dppm) as **P2**, the trinuclear tri(sulfido) cluster $[(Cp^*Ir)\{Re(L)\}_2(\mu_3\text{-}S)_2(\mu_2\text{-}S)(\mu_2\text{-}dppm)]$ (**9a**) was obtained. Alternatively, this cluster **9a** and its Rh analogue **9b** were derived from the incomplete cubane-type clusters **1a** and **1b** by treatment with dppm. It has also been found that further treatment of the cubane-type cluster **2a** with excess $[Pd(PPh_3)_4]$ affords the heptanuclear tetra(sulfido) cluster $[(Cp^*Ir)\{Pd(PPh_3)\}_4Re_2(\mu_3\text{-}L)_2(\mu_3\text{-}S)_4]$ (**10**). The detailed structures have been determined by the X-ray analyses for **3a**, **6**, **9a**, and **10**.

Introduction

Metal sulfido clusters have been attracting much attention because of their relevance to industrial and biological catalysts.[1] Cubane-type or incomplete cubane-type metal sulfido clusters are of particular interest due to their occurrence at the acive sites in metal−sulfur proteins of biological significance, including, e.g., nitrogenases,[2] hydrogenases,[3] and ferredoxins.[4] We reported previously the stepwise syntheses of trimetallic cubane-type MM′Re_2S_4 clusters (M = Ir, Rh, Ru; M′ = Mo, W, Ru, Rh, Pd), which involve the preparation of bimetallic incomplete cubane-type MRe_2S_4 clusters from a dirhenium complex $[PPh_4]_2[\{ReS(L)\}_2(\mu\text{-}S)_2]$ (L = $S_2C_2(SiMe_3)_2$)[5] and certain metal M species, followed by the incorporation of the other metal M′ fragment into their void corners.[6] For example, incomplete cubane-type cluster $[(Cp^*M)\{Re(L)\}_2(\mu_3\text{-}S)(\mu_2\text{-}S)_3]$ (M = Ir (**1a**), Rh (**1b**); Cp* = η^5-C_5Me_5), obtained by treatment of the dirhenium complex above with $[(Cp^*MCl)_2(\mu\text{-}Cl)_2]$, reacts readily with $[Pd(PPh_3)_4]$ to give the cubane-type cluster $[(Cp^*M)\{Pd(PPh_3)\}\{Re(L)\}_2(\mu_3\text{-}S)_4]$ (M = Ir (**2a**), Rh (**2b**)) (eq 1). These reactions demonstrate a quite versatile method to synthesize numerous trimetallic cubane-type clusters in a rational manner. It is to be noted that precedented reliable routes leading to the tailored trimetallic cubane-type clusters in high yields are quite rare.[7,8]

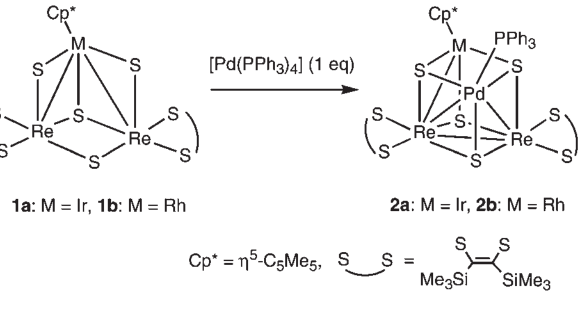

(1)

Cubane-type M_4S_4 cores are generally considered to be of appreciable thermodynamic stability, because much greater

---

*To whom correspondence should be addressed. E-mail: ymizobe@iis.u-tokyo.ac.jp.

[1] (a) Weber, T.; Prins, R.; van Santen, R. A. *Transition Metal Sulphides*; Kluwar Academic Publishers: Dordrecht, The Netherlands, 1998. (b) Stiefel, E. I.; Matsumoto, K. *Transition Metal Sulfur Chemistry: Biological and Industrial Significance*; American Chemical Society: Washington, DC, 1996. (c) Beinert, H.; Holm, R. H.; Münck, E. *Science* **1997**, *277*, 653. (d) Rees, D. C. *Annu. Rev. Biochem.* **2002**, *71*, 221.

[2] (a) Einsle, O.; Tezcan, F. A.; Andrade, S.; Schmid, B.; Yoshida, M.; Howard, J. B.; Rees, D. C. *Science* **2002**, *297*, 1696. (b) Smith, B. E. *Adv. Inorg. Chem.* **1999**, *47*, 159. (c) Howard, J. B.; Rees, D. C. *Chem. Rev.* **1996**, *96*, 2965.

[3] (a) Fontecilla-Camps, J. C.; Volbeda, A.; Cavazza, C.; Nicolet, Y. *Chem. Rev.* **2007**, *107*, 4273. (b) Nicolet, Y.; de Lacey, A. L.; Vernde, X.; Fernandez, V. M.; Hachikian, E. C.; Fontecilla-Camps, J. C. *J. Am. Chem. Soc.* **2001**, *123*, 1596. (c) Peters, J. W.; Lanzilotta, W. N.; Lemon, B. J.; Seefeldt, L. C. *Science* **1998**, *282*, 1853.

Chart 1

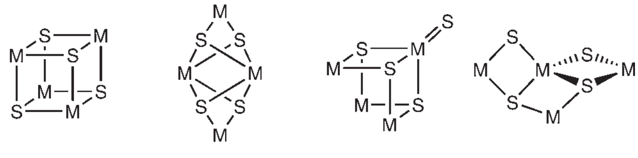

Cubane-type **Raft-type** **Tetrathiometalate-centered**

numbers of these compounds exist than other topological isomers of M_4S_4 cores (Chart 1).[9,10] However, even the cubane-type structures have been sometimes found to be transformed under certain conditions.[1c,11] Elimination or substitution of metal centers,[8,12] desulfurization,[13] and fragmentation into smaller cluster units[14] are known, and sometimes in the latter cases, recombination of the resulting species follows. Small structural modification[15] and extensive rearrangement of two cores into an expanded structure[12a,16] have been also reported. Now, we have found that when cluster **1** is allowed to react with $[\mathrm{Pt(PPh_3)_3}]$ instead of $[\mathrm{Pd(PPh_3)_4}]$, not the cubane-type but the new raft-type tetranuclear tetra(sulfido) clusters are obtained exclusively. Interestingly, treatment of the cubane-type cluster **2a** with a series of diphosphines has also resulted in the formation of the raft-type clusters with the analogous metal and sulfur connecting scheme. It has also been found that **2a** reacts further with $[\mathrm{Pd(PPh_3)_4}]$ to afford the novel heptanuclear $\mathrm{IrPd_4Re_2}$ tetra(sulfido) cluster. Details of the syntheses and structures of these and related new clusters are described below.

Results and Discussion

Reactions of Incomplete Cubane-Type Clusters with $[\mathrm{Pt(PPh_3)_3}]$ to Give Raft-Type Tetranuclear Tetra(sulfido) Clusters. Treatment of **1a** with an equimolar amount of $[\mathrm{Pt(PPh_3)_3}]$ in THF at room temperature resulted in the formation of a raft-type cluster $[(\mathrm{Cp^*Ir})\{\mathrm{Pt(PPh_3)_2}\}\{\mathrm{Re(L)}\}_2(\mu_3\text{-S})_4]$ (**3a**) in moderate yield. The structure of **3a** has been determined in detail by the single-crystal X-ray analysis (vide infra). The Rh analogue $[(\mathrm{Cp^*Rh})\{\mathrm{Pt(PPh_3)_2}\}\{\mathrm{Re(L)}\}_2(\mu_3\text{-S})_4]$ (**3b**) was obtained from $[(\mathrm{Cp^*Rh})\{\mathrm{Re(L)}\}_2(\mu_3\text{-S})(\mu_2\text{-S})_3]$ (**1b**) by analogous treatment, while the reaction of another incomplete cubane-type cluster, $[\{(\mathrm{Pmb})\mathrm{Ru}\}\{\mathrm{Re(L)}\}_2(\mu_3\text{-S})(\mu_2\text{-S})_3]$ (**4**; Pmb = η^6-C_6Me_5H), with $[\mathrm{Pt(PPh_3)_3}]$ also afforded a similar raft-type cluster, $[\{(\mathrm{Pmb})\mathrm{Ru}\}\{\mathrm{Pt(PPh_3)_2}\}\{\mathrm{Re(L)}\}_2(\mu_3\text{-S})_4]$ (**5**) (eq 2). These findings present a sharp contrast to the exclusive formation of cubane-type clusters **2** and $[\{(\mathrm{Pmb})\mathrm{Ru}\}\{\mathrm{Pd(PPh_3)}\}\{\mathrm{Re(L)}\}_2(\mu_3\text{-S})_4]$ from the reactions of $[\mathrm{Pd(PPh_3)_4}]$ with incomplete cubane-type clusters **1** and **4**, respectively, that was reported previously.[6] Total oxidation numbers of metal centers are +13 for both **2** and **3**. However, with respect to the group 10 metal centers, that in **2** exhibits tetrahedral geometry characteristics for Pd^0, while that in **3** is square-planar, typical of $\mathrm{Pt}^{\mathrm{II}}$. These differences observed for the produced tetranuclear clusters may be ascribed to the ability to form stronger M−P bonds and a higher stability at the divalent state displayed by Pt than by Pd.

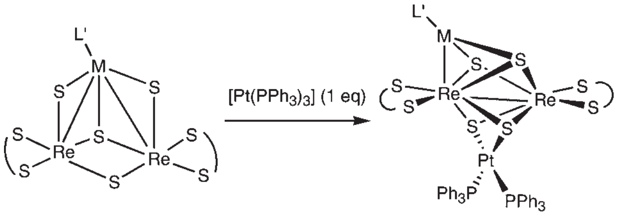

(2)

1a: M = Ir, L' = Cp*
1b: M =Rh, L' = Cp*
4: M = Ru, L' = Pmb
Pmb = η^6-C_6Me_5H

3a: M = Ir, L' = Cp*
3b: M = Rh, L' = Cp*
5: M = Ru, L' = Pmb

In related reactions, Rauchfuss and co-workers observed the formation of either the cubane-type $\mathrm{Fe_2V_2S_4}$ core or the raft-type $\mathrm{PtFeV_2S_4}$ core from the $\mathrm{V_2}(\mu_2\text{-S})_2(\mu_2\text{-S}_2)$ complex with certain Fe or Pt species,[8,17] while Rakowski DuBois et al. obtained the raft-type $\mathrm{Fe_2Mo_2S_4}$ cluster from the $\mathrm{Mo_2}(\mu_2\text{-S})_2(\mu_2\text{-SH})_2$ complex[18] and Curtis et al. derivatized the cubane-type $\mathrm{Ni_2Mo_2S_4}$ cluster from the same complex.[19] These previous findings also

---

(4) (a) Sieker, L. C.; Adman, E.; Jensen, L. H. *Nature* **1972**, *235*, 40. (b) Carter, C. W.; Kraut, J.; Freer, S. T.; Alden, R. A.; Sieker, L. C.; Adman, E.; Jensen, L. H. *Proc. Natl. Acad. Sci. U.S.A.* **1972**, *69*, 3526. (c) Rao, P. V.; Holm, R. H. *Chem. Rev.* **2004**, *104*, 527.

(5) Goodman, J.; Rauchfuss, T. B. *Inorg. Chem.* **1998**, *37*, 5040.

(6) Seino, H.; Kaneko, T.; Fujii, S.; Hidai, M.; Mizobe, Y. *Inorg. Chem.* **2003**, *42*, 4585.

(7) Stepwise synthesis of the cubane-type $\mathrm{WCuMo_2S_4}$ cluster from the $\mathrm{Mo_2S_4}$ complex: Diller, H.; Keck, H.; Wunderlich, H.; Kuchen, W. *J. Organomet. Chem.* **1995**, *489*, 123.

(8) Substitution of one metal center in the cubane-type $\mathrm{V_2Fe_2S_4}$ cluster to form $\mathrm{V_2FeCoS_4}$: Rauchfuss, T. B.; Weatherill, T. D.; Wilson, S. R.; Zebrowski, J. P. *J. Am. Chem. Soc.* **1983**, *105*, 6508.

(9) (a) Harris, S. *Polyhedron* **1989**, *8*, 2843. (b) Sakane, G.; Shibahara, T. In ref, chapter 13. (c) Hernandez-Molina, R.; Sykes, A. G. *Coord. Chem. Rev.* **1999**, *187*, 291. (d) Hernandez-Molina, R.; Sykes, A. G. *J. Chem. Soc., Dalton Trans.* **1999**, 3137. (e) Kuwata, S.; Mizobe, Y.; Hidai, M. *Acc. Chem. Res.* **2000**, *33*, 46.

(10) Examples of tetrathiometalate-centered M_4S_4 structures: (a) Müller, A.; Krickemeyer, E.; Bögge, H. *Z. Anorg. Allg. Chem.* **1987**, *554*, 61. (b) Yuki, M.; Kuge, K.; Okazaki, M.; Mitsui, T.; Inomata, S.; Tobita, H.; Ogino, H. *Inorg. Chim. Acta* **1999**, *291*, 395. (c) Lang, J.-P.; Jiao, C.-M.; Qiao, S.-B.; Zhang, W.-H.; Abrahams, B. F. *Inorg. Chem.* **2005**, *44*, 3664. (d) Huang, Y.-J.; Song, Y.-L.; Chen, Y.; Li, H.-X.; Zhang, Y.; Lang, J.-P. *Dalton Trans.* **2009**, 1411.

(11) In biological systems: (a) Flint, D. H.; Allen, R. M. *Chem. Rev.* **1996**, *96*, 2315. (b) Beinert, H.; Kennedy, M. C.; Stout, C. D. *Chem. Rev.* **1996**, *96*, 2335. (c) Niu, S.; Wang, X.-B.; Yang, X.; Wang, L.-S.; Ichiye, T. *J. Phys. Chem. A* **2004**, *108*, 6750 and references therein.

(12) (a) Coucouvanis, D.; Al-Ahmad, S. A.; Salifoglou, A.; Papaefthymiou, V.; Kostikas, A.; Simopoulos, A. *J. Am. Chem. Soc.* **1992**, *114*, 2472. (b) Mclean, I. J.; Sokolov, M. N.; Hernandez-Molina, R.; Sykes, A. G. *J. Chem. Soc., Dalton Trans.* **2002**, 1941. (c) Koutmos, M.; Coucouvanis, D. *Angew. Chem., Int. Ed.* **2005**, *44*, 1971. (d) Feliz, M.; Llusar, R.; Uriel, S.; Vicent, C.; Brorson, M.; Herbst, K. *Polyhedron* **2005**, *24*, 1212.

(13) (a) Hoh, C.; Holm, R. H. *Inorg. Chim. Acta* **1998**, *270*, 46. (b) Coucouvanis, D.; Han., J.; Moon, N. *J. Am. Chem. Soc.* **2002**, *124*, 216.

(14) (a) Coucouvanis, D.; Kanatzidis, M. G.; Dunham, W. R.; Hagen, W. R. *J. Am. Chem. Soc.* **1984**, *106*, 7998. (b) Kanatzidis, M. G.; Hagen, W. R.; Dunham, W. R.; Lester, R. K.; Coucouvanis, D. *J. Am. Chem. Soc.* **1985**, *107*, 953. (c) Snyder, B. S.; Holm, R. H. *Inorg. Chem.* **1988**, *27*, 2339. (d) Coucouvanis, D.; Al-Ahmad, S.; Kim, C. G.; Mosier, P. E.; Kampf, J. W. *Inorg. Chem.* **1993**, *32*, 1533. (e) Han, J.; Coucouvanis, D. *J. Am. Chem. Soc.* **2001**, *123*, 11304.

(15) (a) Panda, R.; Zhang, Y.; Mclauchlan, C. C.; Rao, P. V.; Tiago de Oliveira, F. A.; Münck, E.; Holm, R. H. *J. Am. Chem. Soc.* **2004**, *126*, 6448. (b) Panda, R.; Berlinguette, C. P.; Zhang, Y.; Holm, R. H. *J. Am. Chem. Soc.* **2005**, *127*, 11092. (c) Sun, J.; Tessier, C.; Holm, R. H. *Inorg. Chem.* **2007**, *46*, 2691.

(16) (a) Zhang, Y.; Holm, R. H. *J. Am. Chem. Soc.* **2003**, *125*, 3910. (b) Zuo, J.-L.; Zhou, H.-C.; Holm, R. H. *Inorg. Chem.* **2003**, *42*, 4624. (c) Zhang, Y.; Holm, R. H. *Inorg. Chem.* **2004**, *43*, 674. (d) Berlinguette, C. P.; Holm, R. H. *J. Am. Chem. Soc.* **2006**, *128*, 11993. (e) Hlavinka, M. L.; Miyaji, T.; Staples, R. J.; Holm, R. H. *Inorg. Chem.* **2007**, *46*, 9192.

(17) (a) Bolinger, C. M.; Rauchfuss, T. B.; Wilson, S. R. *J. Am. Chem. Soc.* **1982**, *104*, 7313. (b) Bolinger, C. M.; Weatherill, T. D.; Rauchfuss, T. B.; Rheingold, A. L.; Day, C. S.; Wilson, S. R. *Inorg. Chem.* **1986**, *25*, 634.

(18) (a) Cowans, B.; Noordik, J.; Rakowski DuBois, M. *Organometallics* **1983**, *2*, 931. (b) Cowans, B. A.; Haltiwanger, R. C.; Rakowski DuBois, M. *Organometallics* **1987**, *6*, 995.

suggest that the produced core structures are highly dependent on the nature of the incorporated metals.

Reactions of 2a with Diphosphines To Give Raft-Type Tetranuclear Tetra(sulfido) Clusters. Stimulated by the occurrence of different cluster core motifs upon changing the nature of the group 10 metal center, alteration of the coordination geometry in **2a** has also been attempted to promote the shape-shift of the core. Interestingly, it has turned out that treatment of the cubane-type cluster **2a** with 1−2 equiv of *cis*-$Ph_2PCH{=}CHPPh_2$ (dppen), $Ph_2PCH_2CH_2PPh_2$ (dppe), and $Ph_2PCH_2CH_2CH_2PPh_2$ (dppp) in THF at room temperature results in facile core rearrangement to afford the raft-type tetranuclear tetra(sulfido) clusters $[(Cp^*Ir)\{Pd(\mathbf{P2})\}\{Re(L)\}_2(\mu_3\text{-}S)_4]$ (**6**, **P2** = dppen; **7**, **P2** = dppe; **8**, **P2** = dppp) analogous to **3** (eq 3).

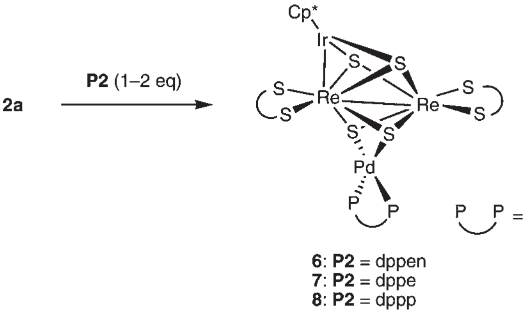

6: **P2** = dppen
7: **P2** = dppe
8: **P2** = dppp

(3)

The structure has been fully determined by the single-crystal X-ray analysis for **6**, whose details are described below together with other clusters. By the strong κ^2-binding of diphosphines, even the Pd center was altered to P_2S_2 coordination via the subsequent rupture of one Pd−(μ_3-S) bond. This caused cluster core rearrangement just as in the formation of **3**. The square-planar geometry indicates that the formal oxidation state of the Pd center has changed from 0 to +2 via the internal redox process, where the total oxidation state of all metal atoms is kept at +13. It is noteworthy that conversion of the cubane-type core into the raft-type requires minimal reorganization,[19b] which is accomplished in this case by the rotation of, e.g., the $PdReS_2$ square by 90° followed by recombination to form two Re−S bonds (eq 4).

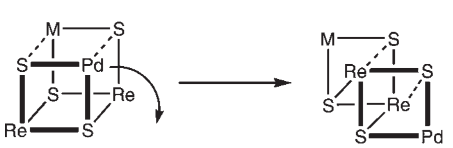

(4)

Holm et al. reported previously the closely related conversion of the tetrahedral Ni^{II} site in $NiFe_3S_4$ cubanes to the planar one by replacing the coordinating PPh_3 with the chelating $Me_2PCH_2CH_2PMe_2$, although cubanoid cores are retained even after the geometry change around Ni.[15]

Formations of Trinuclear Tri(sulfido) Clusters from 2a or 1 with $Ph_2PCH_2PPh_2$ (dppm). Interestingly, when 2 equiv of dppm was reacted with the cubane-type cluster **2a**, the product was proved to be the trinuclear tri(sulfido) cluster $[(Cp^*Ir)\{Re(L)\}_2(\mu_3\text{-}S)_2(\mu_2\text{-}S)(\mu_2\text{-dppm})]$ (**9a**), whose structure has been shown by X-ray crystallography (Scheme 1). Concurrent formation of $Ph_2P({=}S)CH_2PPh_2$ (dppmS) and free PPh_3 was confirmed, but the fate of Pd was unclear.

Scheme 1

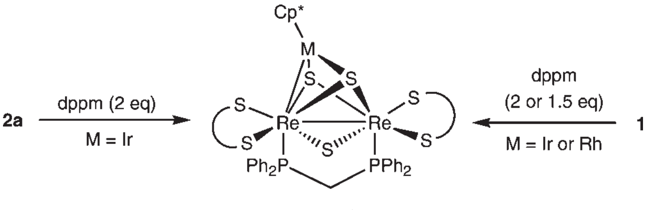

9a: M = Ir
9b: M = Rh

As expected, **9a** was obtained more cleanly from the reaction of incomplete cubane-type trinuclear cluster **1a** with 2 equiv of dppm (Scheme 1), where the NMR spectra of the reaction mixture demonstrated the formation of **9a** and dppmS in a ratio of 1:0.9 together with a small amount of $Ph_2P({=}S)CH_2P({=}S)Ph_2$ ($dppmS_2$). Charging a lesser amount of dppm resulted in an increase of $dppmS_2$ and decrease of dppmS. When equimolar amounts of **1a** and dppm were reacted, $^{31}P\{^1H\}$ NMR signals for only **9a** and $dppmS_2$ (ca. 1:1) were observed, and neither dppm nor dppmS existed. The ^1H NMR spectrum of this reaction mixture indicated the absence of **1a** and the formation of some other cluster products containing no phosphorus ligands. From these observations, a plausible mechanism of the reaction between **1a** and dppm is considered in which **1a** transfers one S atom to dppm or dppmS and the resulting trisulfido cluster is captured by dppm. The formal oxidation number of metal atoms is reduced by 2 in total as the result of S atom elimination. The μ_2-binding of dppm is probably suitable for stabilizing this trisulfido core. Although even dppe desulfurized **1a** to form the corresponding phosphine sulfide, the cluster species, which was estimated to be the dppe adduct,[20] was not cleanly produced in spite of the presence of excess dppe. The ^1H NMR signals of the other products in this reaction were identical to those of the byproducts in the reaction with an insufficient amount of dppm. It has also been found that its Rh congener $[(Cp^*Rh)\{Re(L)\}_2(\mu_3\text{-}S)_2(\mu_2\text{-}S)(\mu_2\text{-dppm})]$ (**9b**) is available by treatment of $[(Cp^*Rh)\{Re(L)\}_2(\mu_3\text{-}S)(\mu_2\text{-}S)_3]$ (**1b**) with 1.5 equiv of dppm, whereas the $RuRe_2S_4$ cluster **4** afforded a mixture of intractable products under similar reaction conditions.

The reaction of **2a** with dppm was slower than that of **1a**. In the reactions with 2 equiv of dppm at room temperature, **2a** still remained after 46 h (**2a**/**9a** ~ 1:4), while **1a** was consumed within 18 h. Similarly to other diphosphines, dppm presumably substitutes the PPh_3 ligand in **2a**, but its lesser ability for κ^2-coordination obstructs the shape shift of the cluster. One probable route to **9a** is that the noncoordinated PPh_2 group of the κ^1-bound dppm abstracts an S atom in the cluster core, followed by the release of Pd^0 species from the resulting cluster and coordination of another dppm.

---

[19] (a) Curtis, M. D.; Williams, P. D. *Inorg. Chem.* **1983**, *22*, 2661. (b) Curtis, M. D.; Williams, P. D.; Butler, W. M. *Inorg. Chem.* **1988**, *27*, 2853.

[20] This species exhibited the following NMR signals but could not be fully characterized. ^1H NMR (C_6D_6): δ 0.21, 0.45 (s, 9H each, $SiMe_3$), 0.89 (s, 18H, $SiMe_3$), 1.45 (s, 15H, Cp*). $^{31}P\{^1H\}$ NMR (C_6D_6): δ 14.1, 36.7 (d, $J_{PP'}$ = 3 Hz).

Preparation of Heptanuclear Tetra(sulfido) Cluster from 2a and [Pd(PPh$_3$)$_4$]. When the cubane-type cluster **2a** was treated with 3 equiv of [Pd(PPh$_3$)$_4$] in THF at room temperature, incorporation of Pd fragments proceeded further to give the heptanuclear tetra(sulfido) cluster [(Cp*Ir){Pd(PPh$_3$)}$_4${Re(L)}$_2$(μ_3-S)$_4$] (**10**) in moderate yield (eq 5), the structure of which has been determined using X-ray analysis. While all metal atoms are bridged only by μ_3-sulfido ligands in other IrPdRe$_2$S$_4$ clusters of both cubane-type **2a** and raft-type **6**−**8**, two dithiolates L's act as bridging ligands to bind excess Pd centers in **10**. Each Pd atom is connected to a Re center with one μ_3-S and one S atom in L, and such a coordination style has been precedented in Mo/S/Cu clusters.[21] The reactions with less than 3 equiv of [Pd(PPh$_3$)$_4$] gave mixtures of **10** and **2a**, and no other intermediary compounds were obtained or detected, as indicated by the NMR study. It might be noteworthy that the analogous treatment of **2a** with 3 equiv of [Pt(PPh$_3$)$_3$] resulted in conversion into a mixture of **3a** and **10** together with one uncharacterized complex, while **3a** did not react further with [Pt(PPh$_3$)$_3$]. Although the reaction pathway from **2a** to **10** cannot be proposed definitely, binding of a Pd(PPh$_3$) unit to the S atom of L is considered to trigger the cluster deformation, which extrudes the Pd center in the cubane-type core to the outside.

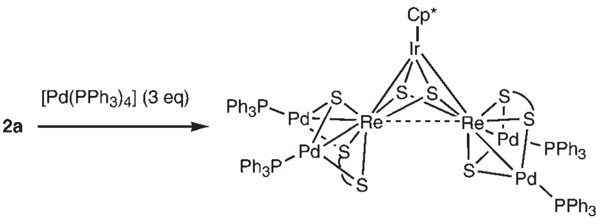

10

(5)

In summary, transformations of metal sulfido cluster cores starting from those of the cubane type and incomplete cubane type have been demonstrated. It is noteworthy that even the cubane-type cores are readily converted to those with different structures, depending on the nature of the metals and ligands incorporated. Because these transformations are always accompanied by the cleavage of Ir−S and Pd−S bonds, a flexible geometry change of these metals is presumed to play another important role.

Structure Determination of the Clusters. The ORTEP drawings of the raft-type tetranuclear tetrasulfido clusters **3a** and **6** are shown in Figures 1 and 2, respectively, while the selected interatomic distances and angles therein are listed in Table 1.

Both clusters have almost planar IrMRe$_2$ metal cores (M = Pt (**3a**) or Pd (**6**)) that correspond to the pseudo mirror plane. For these metal cores, the deviations of the positions of metal centers from the least-squares planes defined by four metals are less than 0.07 Å in **3a** and 0.01 Å in **6**. The observed intermetallic distances indicate that metal−metal bonding interactions are present only between two Re atoms with distances at 2.6437(5) and 2.6476(4) Å and between Re(1) and Ir at 2.8147(3) and 2.7758(3) Å for **3a** and **6**, which are much shorter than all other metal−metal separations (>3.4 Å). If these metal−metal bonds are ignored, the geometries around Re, Ir, and M are essentially a trigonal prism, two-legged piano-stool, and square plane, respectively. Four sulfido ligands bind to the triangular IrRe$_2$ and MRe$_2$ units from both sides in a μ_3 manner, where the Re−S bonds (2.40−2.46 Å) are significantly longer than the Ir−S and M−S bonds (2.27−2.34 Å). The M−S and M−P distances compare well with those of the square-planar Pd^{II} and Pt^{II} complexes with *cis*-S$_2$P$_2$ ligand configuration.[22] Including these, all corresponding metrical parameters associated with the IrMRe$_2$S$_4$ cores in **3a** and **6** are almost identical, except for the bond angles around M, for which the P−Pt−P angle with bulky monophosphine PPh$_3$ in **3a** (102.29(7)°) is much wider than the P−Pd−P angle with the dppen ligand forming a five-membered chelating ring in **6** (85.24(8)°).

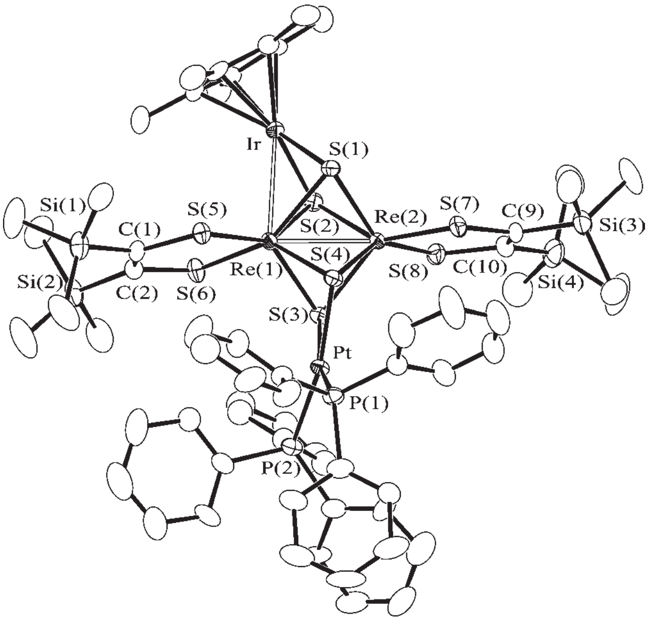

Figure 1. An ORTEP drawing for **3a** at the 30% probability level. All hydrogen atoms and the three disordered Ph groups with lower occupancies are omitted for clarity.

The NMR data are consistent with these structures. Thus, the protons in SiMe$_3$ groups are recorded as two singlets, since two dithiolate ligands L's are not equivalent due to the tilt of the Ir center to the direction of Re(1), while two SiMe$_3$ groups in each L are equivalent. Accordingly, the ^{31}P NMR spectra exhibit only one resonance because of the equivalence of two P atoms. The VT-^{1}H NMR study for **3a** has shown that the two signals due to SiMe$_3$ protons coalesce at 70 °C and are recorded as one broad signal at 90 °C, indicating that the Ir−Re bond migration is taking place rapidly at higher temperatures. Such bond migration was observed also for **3b** and **8**, although it is somewhat slower in these clusters than in **3a**.

The crystallographic structure of **9a** is depicted in Figure 3, while important metrical parameters are summarized in Table 2. Cluster **9a** has a triangular core, for which the metal−metal bonding interactions are present between two Re atoms and between Re(1) and Ir. The

---

[21] (a) Wei, Z.-H.; Li, H.-X.; Zhang, W.-H.; Ren, Z.-G.; Zhang, Y.; Lang, J.-P.; Abrahams, B. F. *Inorg. Chem.* **2008**, *47*, 10461. (b) Li, J.-J.; Duan, T.; Zhang, Q.-F.; Leung, W.-H. *Chem. Lett.* **2009**, *38*, 506.

[22] Reference 15b and those cited therein.

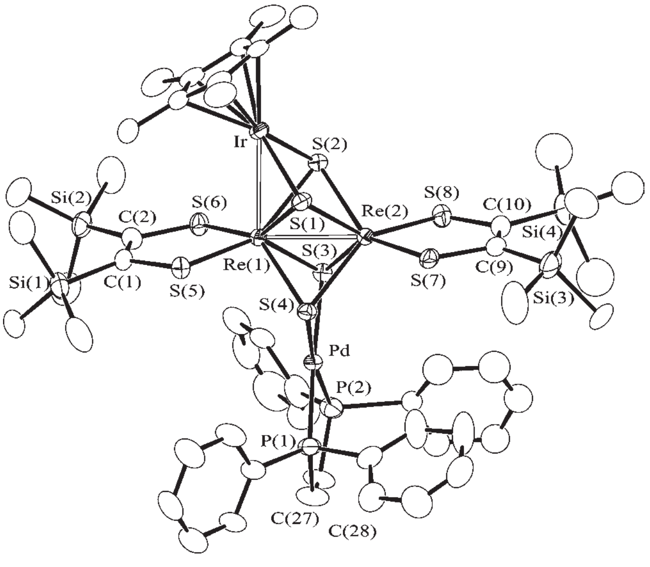

Figure 2. An ORTEP drawing for **6** at the 30% probability level. All hydrogen atoms as well as the disordered Me and Ph groups with lower occupancies are omitted for clarity.

Table 1. Selected Interatomic Distances (Å) and Angles (deg) in **3a** and **6**

	3a (M = Pt)	**6** (M = Pd)
	(a) Distances	
Re(1)−Re(2)	2.6437(5)	2.6476(4)
Re(1)−Ir	2.8147(3)	2.7758(3)
Re(2)$\cdots$Ir	3.6864(4)	3.7232(4)
Re(1)$\cdots$M	3.4361(3)	3.4503(6)
Re(2)$\cdots$M	3.6166(3)	3.5532(6)
Re(1)−S (μ_3-S)	2.414(2)—2.457(2)	2.416(2)—2.444(2)
Re(1)−S (L)	2.302(2), 2.298(2)	2.300(2), 2.298(2)
Re(2)−S (μ_3-S)	2.400(2)—2.440(2)	2.406(2)—2.434(2)
Re(2)−S (L)	2.284(2), 2.285(2)	2.292(2), 2.292(2)
Ir−S	2.275(2), 2.310(2)	2.311(2), 2.297(2)
M−S	2.339(2), 2.313(2)	2.327(2), 2.315(2)
M−P	2.306(2), 2.291(2)	2.283(2), 2.278(2)
	(b) Angles	
Re(2)−Re(1)−Ir	84.90(1)	86.68(1)
S(1)−Ir−S(2)	78.69(7)	78.12(7)
S(3)−M−S(4)	75.78(7)	76.89(6)
P(1)−M−P(2)	102.27(7)	85.24(8)
S−M−P (cis)	88.34(7), 94.28(7)	97.72(7), 99.61(7)

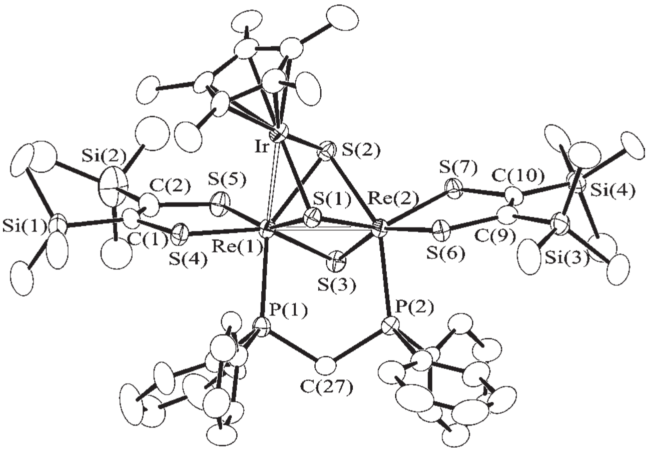

Figure 3. An ORTEP drawing for **9a** at the 30% probability level. All hydrogen atoms as well as the disordered Me_3Si group with lower occupancy are omitted for clarity.

Table 2. Selected Interatomic Distances (Å) and Angles (deg) in **9a**

	(a) Distances		
Re(1)−Re(2)	2.7779(7)	Re(1)−Ir	2.8387(4)
Re(2)$\cdots$Ir	3.5734(6)		
Re(1)−S(1)	2.435(2)	Re(1)−S(2)	2.410(2)
Re(1)−S(3)	2.412(2)	Re(1)−S(4)	2.311(2)
Re(1)−S(5)	2.285(2)	Re(1)−P(1)	2.432(2)
Re(2)−S(1)	2.384(2)	Re(2)−S(2)	2.416(2)
Re(2)−S(3)	2.382(2)	Re(2)−S(6)	2.309(2)
Re(2)−S(7)	2.310(2)	Re(2)−P(2)	2.385(2)
Ir−S(1)	2.293(2)	Ir−S(2)	2.300(2)
	(b) Angles		
Re(2)−Re(1)−Ir	79.01(2)	S(1)−Re(1)−S(2)	76.48(7)
S(2)−Re(1)−S(3)	75.52(7)	S(1)−Re(2)−S(2)	77.33(7)
S(2)−Re(2)−S(3)	75.97(7)	S(1)−Ir−S(2)	81.55(7)

Re(1)−Re(2) and Re(1)−Ir bonds are somewhat elongated from those in **3a** and **6**, while the Re(2)$\cdots$Ir separation is considerably smaller.[23] This triangular core is capped from both sides with two μ_3-sulfido ligands, and the Re−Re bond is further bridged by one μ_2-S and one μ_2-dppm. The Ir−S bonds are shorter than the Re−S(sulfido) bonds significantly, while the Re−μ_3-S and Re−μ_2-S bond lengths are essentially the same. Neglecting the metal−metal bonds described above, the geometry around the Ir atom is two-legged piano-stool, and that around the Re atom is a twisted trigonal prism. For the Re(1) center, the three edges joining the triangular bases are S(1)−S(2), P(1)−S(3), and S(4)−S(5), whose twist (trigonal distortion) angles ϕ are ca. 20°, 35°, and 17°, respectively.[24] Those for the Re(2) center are S(1)−S(2), P(2)−S(3), and S(6)−S(7) with $\phi \sim 16°, 44°$, and 8°, respectively. The dithiolene ring formed from the Re(2) atom and L is slightly folded along the S−S axis by 12.2(2)° toward the direction of P(2), while the other dithiolene ring in **9a** as well as those in **3a** and **6** are of good planarity (fold angles at 0.4(3)−4.7(2)°).

Since $^{31}P\{^1H\}$ NMR spectra of **9a** and **9b** exhibited only one singlet, it is presumed that the rapid Re−Ir bond migration is taking place in a solution state for these clusters. The VT-^{1}H NMR study for **9a** in toluene-d_8 (−80 to +80 °C) has indicated further that this motion of the Cp*Ir unit is quite rapid even at low temperatures, since the two singlet signals due to the TMS methyl protons are essentially unaltered even at −80 °C. On the other hand, some broadening of these signals at temperatures higher than 60 °C suggests the occurrence of pseudorotation of the dithiolene rings in this temperature range. Dynamic motions due to metal−metal bond migration and pseudorotation of the dithiolene ring have been also observed for **1a** and **2a**, as well as analogous cubane-type and incomplete cubane-type clusters, and they are speculated to be linked with the geometrical change of the five-coordinated Re centers.[6] Although the Re centers in **9a** are six-coordinated, no geometrical change

---

[23] Distances of quadruply bridged M−M bonds tend to be smaller than those of triply bridged ones: Rakowski Dubois, M.; Jagirdar, B. R.; Dietz, S.; Noll, B. C. *Organometallics* **1997**, *16*, 294.

[24] (a) Stiefel, E. I.; Brown, G. F. *Inorg. Chem.* **1972**, *11*, 434. (b) Eisenberg, R.; Brennessel, W. W. *Acta Crystallogr. Sect. C* **2006**, *C62*, m464. (c) Sproules, S.; Benedito, F. L.; Bill, E.; Weyhermüller, T.; George, S. D.; Wieghardt, K. *Inorg. Chem.* **2009**, *48*, 10926.

Table 3. Selected Interatomic Distances (Å) and Angles (deg) in **10**

(a) Distances

Re(1)···Re(2)	3.0213(4)		
Re(1)−Ir	2.8326(4)	Re(2)−Ir	2.8015(4)
Re−Pd	2.7041(7)−2.7285(8)		
Pd(1)···Pd(2)	3.185(1)	Pd(3)···Pd(4)	3.127(1)
Re−S(−Ir)	2.343(2)−2.384(2)		
Re(1)−S(3)	2.251(2)	Re(2)−S(4)	2.256(2)
Re−S (L)	2.342(2)−2.363(3)		
Ir−S(1)	2.300(3)	Ir−S(2)	2.313(2)
Pd−S (μ_3-S)	2.286(2)−2.315(2)		
Pd−S (L)	2.342(2)−2.364(2)		
Pd−P	2.250(2)−2.271(3)		

(b) Angles

Re(1)−Ir−Re(2)	64.86(1)	Ir−Re(1)−Re(2)	57.074(9)
Ir−Re(2)−Re(1)	58.07(1)	Pd(1)−Re(1)−Pd(2)	71.80(2)
Pd(3)−Re(2)−Pd(4)	70.50(2)	S(1)−Ir−S(2)	91.41(8)
S−Pd−S	107.19(8)−107.93(8)		
P−Pd−S (μ_3-S)	114.91(8)−122.52(8)		
P−Pd−S (L)	130.16(8)−134.49(9)		

is necessary for exchange of the Ir−Re bond. The more rapid motion of **9a** than **3** and **8** is ascribable to long Ir−Re bond and short Ir···Re nonbond distances in comparison with **3a** and **6**.

As shown in Figure 4 and Table 3, **10** has an $IrPd_4Re_2$ core, where two triangular $RePd_2$ fragments are connected to Ir with the Ir−Re bonds at 2.8326(4) and 2.8015(4) Å. The Re−Re distance at 3.0213(4) Å might suggest the presence of some interactions between two Re atoms, but it is very weak if there at all. The Re−Pd distances at 2.70−2.73 Å fall in the range of metal−metal single bonds, while the Pd···Pd separations of 3.185(1) and 3.127(1) Å may suggest the absence of Pd−Pd bonds. There is a pseudomirror plane containing the central $IrRe_2$ triangle, and it passes through each midpoint of two mutually adjacent Pd atoms. Two sulfides bind to the $IrRe_2$ triangle from both sides in a μ_3-manner. The Re(1)Pd(1)Pd(2) triangle is almost parallel to the Re(1)−Re(2) vector and capped by one μ_3-sulfido at the side near Ir. The sulfido cap of the Re(2)Pd(3)Pd(4) triangle, which is parallel to the Re(2)−Ir edge, is at the side close to Re(1). At the side opposite the μ_3-sulfido ligand, the Pd−S bonds are also present between each of the Pd atoms and the dithiolate S atom in the vicinity. The Re−S bonds of these bridging L's are slightly elongated in comparison with the nonbridging L's in other clusters (2.28−2.32 Å), although the Re−L dithiolene rings remain considerably planar. Folding angles along the S−S axis are only 10.0(3)° and 7.2(3)° for those associated with Re(1) and Re(2), and both of them are folded toward the Pd atoms. The geometry around Ir is a two-legged piano-stool, and that around Pd is severely distorted trigonal-planar. Each Re center has a square-pyramid structure with S(3) or S(4) at the apical position, whose Re−S bond is shorter than others of basal S atoms. The S−Re−S bond angles between the apical and the basal positions are 103.66(8)−110.00(7)°, and those of the neighboring two basal S atoms are 82.59(9)−89.05(7)°. The NMR spectra exhibiting two TMS proton signals and two ^{31}P signals are consistent with the solid state structure.

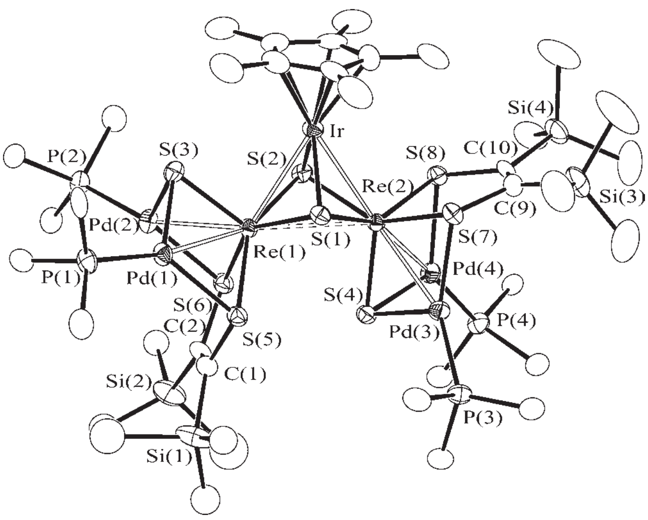

Figure 4. ORTEP drawing for **10** at the 30% probability level. Only ipso-carbon atoms are shown for phenyl groups, and all hydrogen atoms as well as the disordered Me groups with lower occupancies are omitted for clarity.

Description of Redox Properties. Electrochemical measurements of representative clusters have been performed by cyclic voltammetry, and their redox potentials are summarized in Table 4. Incomplete cubane-type cluster **1a** and cubane-type cluster **2a** showed two oxidative and two reductive couples, which were all reversible except for a quasi-reversible second oxidation of **1a**. It is clearly indicated that incorporation of a Pd^0 center has caused the shift of redox potentials toward the negative direction. Raft-type cluster **3a** and trisulfido cluster **9a**, in which the $IrRe_2$ moieties are formally at the +11 oxidation state, are easier to oxidize than **2a**. Contrarily, the reduction processes of these two clusters are irreversible and much harder than those of **1a** and **2a**. Although redox properties of the raft-type $IrPdRe_2S_4$ clusters were found to be similar to that of **3a**, reliable potential values were not obtained due to very low solubility. The first oxidation process of **10** was irreversible, but four reversible oxidation waves were observed thereafter within a range of 0.8 V.

Experimental Section

General. All manipulations were carried out under N_2 using standard Schlenk techniques. Solvents were dried by common methods and distilled under N_2 before use. Complexes **1**, **2**, **4**,[6] $[Pd(PPh_3)_4]$,[25] and $[Pt(PPh_3)_3]$[26] were prepared according to the literature methods, while other chemicals were obtained commercially and used as received.

NMR spectra were measured on a JEOL alpha-400 spectrometer, whereby the chemical shifts were referenced to the signal of C_6HD_5 at δ 7.15. Elemental analyses were done with a Perkin-Elmer 2400 series II CHN analyzer. Electrochemical measurements were performed with a BAS CV-50W electrochemical analyzer using a glassy carbon working electrode, a Pt wire counter electrode, and an SCE as a reference. Potentials were measured in a 0.1 M THF solution of $[Bu^n{}_4N][BF_4]$ at a scan rate of 200 mV/s. Elemental analyses were done with a Perkin-Elmer 2400 series II CHN analyzer.

Preparation of 3a. Compound **1a** (65 mg, 0.050 mmol) and $[Pt(PPh_3)_3]$ (49 mg, 0.050 mmol) were charged in a Schlenk tube, and THF (5 mL) was added. The mixture was stirred at room temperature for 18 h, and the resultant dark green-brown mixture was filtered. The filtrate was concentrated to ca. 2 mL, and hexane was layered on it. After 10 days, dark brown crystals of

---

(25) Coulson, D. R. *Inorg. Synth.* **1972**, *13*, 121.
(26) Ugo, R.; Cariari, F.; La Monica, G. *Inorg. Synth.* **1968**, *11*, 105.

Table 4. Redox Potentials for **1a**, **2a**, **3a**, **9a**, and **10**

	$E_{1/2}$/V (vs ferrocene/ferrocenium couple)[a]			
cluster	−2/−1	−1/0	0/+1	+1/+2
1a	−1.47 (rv)	−1.22 (rv)	−0.09 (rv)	+0.34 (qr)
2a	−1.80 (rv)	−1.52 (rv)	−0.18 (rv)	+0.12 (rv)
3a		−2.37 (ir)	−0.39 (rv)	+0.16 (qr)
9a		−1.86 (ir)	−0.62 (rv)	−0.30 (rv)
10		−2.34 (ir)	−0.38 (ir)	−0.37, −0.13, +0.15, +0.40 (rv)[b]

[a] rv, reversible; qr, quasi-reversible; ir, irreversible. For irreversible redox, peak potentials are shown. [b] Four sequential one-electron oxidations.

3a·THF precipitated, which were filtered off and dried in vacuo (80 mg, 76% yield). ^{1}H NMR (C_6D_6): δ 0.71, 0.84 (s, 18H each, $SiMe_3$), 1.66 (s, 15H, Cp*), 6.80−6.90 (m, 18H, Ph), 7.15−7.25 (m, 12H, Ph), 1.41, 3.57 (m, 4H each, THF). $^{31}P\{^1H\}$ NMR (C_6D_6): δ 31.4 (s with ^{195}Pt satellites, J_{Pt-P} = 2820 Hz). Anal. Calcd for $C_{66}H_{89}IrOP_2PtRe_2S_8Si_4$: C, 37.95; H, 4.29. Found: C, 37.94; H, 4.26.

Preparation of 3b. This complex was obtained similarly from **1b** (62 mg, 0.051 mmol) and $[Pt(PPh_3)_3]$ (50 mg, 0.051 mmol) as dark green crystals of **3b**·THF in 46% yield (46 mg). ^{1}H NMR (C_6D_6): δ 0.71, 0.86 (s, 18H each, $SiMe_3$), 1.57 (s, 15H, Cp*), 6.8−6.9 (m, 18H, Ph), 7.1−7.2 (m, 12H, Ph), 1.41, 3.57 (m, 4H each, THF). $^{31}P\{^1H\}$ NMR (C_6D_6): δ 30.7 (s with ^{195}Pt satellites, J_{Pt-P} = 2834 Hz). Anal. Calcd for $C_{66}H_{89}OP_2PtRe_2RhS_8Si_4$: C, 39.64; H, 4.49. Found: C, 40.01; H, 4.41.

Preparation of 5. Compound **4** (66 mg, 0.051 mmol) and $[Pt(PPh_3)_3]$ (50 mg, 0.051 mmol) were charged in a Schlenk tube, and THF (5 mL) was added at 0 °C. The mixture was stirred at this temperature for 18 h, and the resultant mixture was filtered. Hexane was added to the concentrated filtrate, which was kept at −20 °C to give **5** as black microcrystals (71 mg, 69% yield). ^{1}H NMR (C_6D_6): δ 0.74, 0.86 (s, 18H each, $SiMe_3$), 1.61 (s, 6H, C_6Me), 1.64 (s, 3H, C_6Me), 1.66 (s, 6H, C_6Me), 4.36 (s, 1H, C_6H), 6.8−6.9 (m, 18H, Ph), 7.1−7.2 (m, 12H, Ph). $^{31}P\{^1H\}$ NMR (C_6D_6): δ 30.6 (s with ^{195}Pt satellites, J_{Pt-P} = 2815 Hz). Anal. Calcd for $C_{63}H_{82}P_2PtRe_2RuS_8Si_4$: C, 39.03; H, 4.26. Found: C, 38.84; H, 4.19.

Preparation of 6. Into a THF solution (5 mL) of **2a** (82 mg, 0.049 mmol) was added dppen (41 mg, 0.10 mmol), and the mixture was stirred at room temperature for 20 h. The resultant dark green mixture was filtered to give **6** as green-brown microcrystals, which were washed with a small amount of THF and dried in vacuo (20 mg, 22% yield). The addition of MeCN to the filtrate afforded another crop of **6** as dark green crystals of **6**·0.8MeCN (12 mg, 14% yield). For **6**·0.8MeCN, ^{1}H NMR (C_6D_6): δ 0.68, 0.71 (s, 18H each, $SiMe_3$), 1.71 (s, 15H, Cp*), 6.15−6.35 (m, 2H, CH=CH), 7.0−7.1 (m, 12H, Ph), 7.1−7.3 (m, 8H, Ph), 0.57 (s, ca. 2.5H, MeCN). $^{31}P\{^1H\}$ NMR (C_6D_6): δ 54.0 (s). Anal. Calcd for $C_{53.6}H_{75.4}IrN_{0.8}P_2PdRe_2S_8Si_4$: C, 35.12; H, 4.15; N, 0.61. Found: C, 35.08; H, 4.24; N, 0.59.

Preparation of 7. Into a solution of **2a** (79 mg, 0.048 mmol) in THF (3 mL) was added dppe (30 mg, 0.075 mmol) dissolved in THF (0.5 mL), and the mixture was stirred at room temperature for 70 h. The product **7**·0.5THF precipitated as dark green-brown crystals, which were filtered off, washed with a small portion of THF, and dried in vacuo (64 mg, 74% yield). ^{1}H NMR (C_6D_6): δ 0.716, 0.720 (s, 18H each, $SiMe_3$), 1.15−1.4 (m, 4H, PCH_2), 1.73 (s, 15H, Cp*), 6.95−7.1 (m, 12H, Ph), 7.3−7.4, 7.4−7.5 (m, 4H each, Ph), 1.41, 3.57 (m, 2H each, THF). $^{31}P\{^1H\}$ NMR (C_6D_6): δ 46.1 (s). Anal. Calcd for $C_{54}H_{79}IrO_{0.5}P_2PdRe_2S_8Si_4$: C, 35.29; H, 4.33. Found: C, 35.43; H, 4.28.

Preparation of 8. Analogous treatment of **2a** (81 mg, 0.049 mmol) with dppp (20 mg, 0.047 mmol) afforded **8** as black microcrystals (41 mg, 47% yield). ^{1}H NMR (C_6D_6): δ 0.70, 0.77 (s, 18H each, $SiMe_3$), 0.9−1.5 (m, 6H, CH_2), 1.70 (s, 15H, Cp*), 6.9−7.3 (m, 20H, Ph). $^{31}P\{^1H\}$ NMR (C_6D_6): δ 8.8 (s). Anal. Calcd for $C_{53}H_{77}IrP_2PdRe_2S_8Si_4$: C, 35.05; H, 4.27. Found: C, 35.37; H, 4.26.

Table 5. Crystal Data for **3a**·THF, **6**·0.8MeCN, **9a**, and **10**

	3a·THF	**6**·0.8MeCN
formula	$C_{66}H_{89}IrOP_2PtRe_2S_8Si_4$	$C_{53.6}H_{75.4}IrN_{0.8}P_2PdRe_2S_8Si_4$
fw	2088.92	1832.79
space group	*C*2/*c* (No. 15)	*Pbca* (No. 61)
a, Å	31.430(4)	20.0952(7)
b, Å	18.408(2)	21.5969(8)
c, Å	30.172(4)	31.319(1)
α, deg	90	90
β, deg	114.3360(5)	90
γ, deg	90	90
V, Å^3	15905(3)	13592.2(8)
Z	8	8
ρ_{calcd}, g cm^{-3}	1.745	1.791
cryst size, mm^3	0.40 × 0.15 × 0.10	0.40 × 0.15 × 0.05
no. of unique reflns	18929	16077
no. of data ($I > 2\sigma(I)$)	10801	9817
no. of variables	855	732
transmn factor	0.107−0.506	0.441−0.735
R1[a]	0.039	0.043
wR2[b]	0.134	0.132
GOF[c]	1.039	1.029

	9a	**10**
formula	$C_{51}H_{73}IrP_2Re_2S_7Si_4$	$C_{98}H_{111}IrP_4Pd_4Re_2S_8Si_4$
fw	1649.48	2771.91
space group	$P2_12_12_1$ (No. 19)	$P\bar{1}$ (No. 2)
a, Å	9.9237(2)	15.550(4)
b, Å	11.3495(3)	15.646(4)
c, Å	56.910(2)	24.209(6)
α, deg	90	71.615(7)
β, deg	90	81.275(10)
γ, deg	90	75.918(9)
V, Å^3	6409.7(3)	5403(2)
Z	4	2
ρ_{calcd}, g cm^{-3}	1.709	1.704
cryst size, mm^3	0.30 × 0.15 × 0.10	0.30 × 0.20 × 0.05
no. of unique reflns	11312	25484
no. of data ($I > 2\sigma(I)$)	10781	18411
no. of variables	676	1177
transmn factor	0.398−0.536	0.501−0.802
R1[a]	0.035	0.063
wR2[b]	0.102	0.149
GOF[c]	1.040	1.013

[a] $R1 = \sum||F_o| - |F_c||/\sum|F_o|$ ($I > 2\sigma(I)$). [b] $wR2 = [\sum(w(F_o^2 - F_c^2)^2)/\sum w(F_o^2)^2]^{1/2}$ (all data). [c] $GOF = [\sum w(|F_o| - |F_c|)^2/\{(\text{no. observed}) - (\text{no. variables})\}]^{1/2}$.

Preparation of 9a from 2a. Into a solution of **2a** (82 mg, 0.049 mmol) in THF (5 mL) was added dppm (39 mg, 0.10 mmol), and the mixture was stirred at room temperature for 46 h. Addition of MeCN to the filtrate of the reaction mixture afforded **9a** as black crystals (20 mg, 24% yield). ^{1}H NMR (C_6D_6): δ 0.45, 0.56 (s, 18H each, $SiMe_3$), 1.41 (s, 15H, Cp*), 1.83 (dt, 1H, *J* = 13.7 and 4.5 Hz, PCH_2), 4.05 (br q, 1H, *J* = 13 Hz, PCH_2), 6.7−7.0 (m, 16H, Ph), 7.7−7.8 (m, 4H, Ph). $^{31}P\{^1H\}$ NMR (C_6D_6): δ −18.7 (s). Anal. Calcd for $C_{51}H_{73}IrP_2Re_2S_7Si_4$: C, 37.14; H, 4.46. Found: C, 37.14; H, 4.38.

Preparation of 9a from 1a. A mixture of **1a** (260 mg, 0.200 mmol) and dppm (153 mg, 0.399 mmol) in THF (20 mL) was stirred at room temperature for 18 h. The NMR spectra of the reaction mixture showed the presence of **9a** and dppmS in a ratio of 1:0.9 together with a small amount of $dppmS_2$. The mixture was filtered, and MeCN (40 mL) was added to the filtrate. Slow evaporation of volatiles under a vacuum to a volume of ca. 20 mL afforded **9a** as black crystals, which were filtered off, washed with a small amount of MeCN, and then dried in vacuo (288 mg, 87% yield).

Preparation of 9b from 1b. Cluster **9b** was obtained analogously from **1b** (61 mg, 0.050 mmol) and dppm (28 mg, 0.074 mmol) in 37% yield as black crystals. ^{1}H NMR (C_6D_6): δ 0.48, 0.58 (s, 18H each, $SiMe_3$), 1.29 (s, 15H, Cp*), 1.84 (dt, 1H, J = 13.6 and 4.4 Hz, PCH_2), 4.00 (br q, 1H, J = 13 Hz, PCH_2), 6.65−6.95 (m, 16H, Ph), 7.6−7.7 (m, 4H, Ph). ^{31}P{^{1}H} NMR (C_6D_6): δ −14.4 (s). Anal. Calcd for $C_{51}H_{73}RhP_2Re_2S_7Si_4$: C, 39.26; H, 4.72. Found: C, 39.35; H, 4.71.

Preparation of 10. A mixture of **2a** (25 mg, 0.015 mmol) and [Pd(PPh_3)$_4$] (53 mg, 0.046 mmol) was dissolved in THF (5 mL), and the solution was stirred at room temperature for 17 h. The resultant mixture was filtered, and the filtrate was concentrated. Addition of MeCN afforded **10** as dark brown crystals (26 mg, 62% yield). ^{1}H NMR (C_6D_6): δ 0.15, 0.34 (s, 18H each, $SiMe_3$), 1.98 (s, 15H, Cp*), 6.8−7.7 (m, 60H, Ph). ^{31}P{^{1}H} NMR (C_6D_6): δ 32.4, 34.7 (s, 2P each). Anal. Calcd for $C_{98}H_{111}IrP_4Pd_4Re_2S_8Si_4$: C, 42.46; H, 4.04. Found: C, 42.29; H, 4.04.

X-Ray Crystallography. Single crystals of **3a**·THF, **6**·0.8MeCN, **9a**, and **10** were sealed in glass capillaries under argon and mounted on a Rigaku Mercury-CCD diffractometer equipped with a graphite-monochromatized Mo Kα source. All diffraction studies were done at 23 °C, and the details are listed in Table 5. Data collection was performed by using the CrystalClear program package.[27] All data were corrected for absorption.

Structure solution and refinements were conducted by using the CrystalStructure program package.[28] The positions of non-hydrogen atoms were determined by Patterson methods (PATTY)[29] and subsequent Fourier synthesis (DIRDIF99).[30] These were refined with anisotropic thermal parameters by full-matrix least-squares techniques, while all hydrogens were placed at the calculated positions and included at the final stages of the refinements. In the crystal of **3a**·THF, the solvating THF is present at the two disordered positions with occupancies of 0.7 and 0.3, which were refined with restraints. The disorder was also observed for three Ph groups in one of the PPh_3 ligands in ratios of 0.50:0.50, 0.60:0.40, and 0.65:0.35, respectively, and the C atoms of less than 0.6 occupancy were refined isotropically. For the crystal of **6**, the amount of solvating MeCN was determined to be 0.8 mol/mol cluster based on the electron densities observed. Disorder was found for the Me groups around Si(3) (0.7:0.3) and Si(4) (0.55:0.45) as well as three Ph groups (0.7:0.3, 0.6:0.4, and 0.55:0.45). The atoms therein with occupancies less than 0.6 were refined isotropically. As for **9a**, only 86% of the total reflections in the range $2\theta < 55°$ were measurable, since crystals of sufficiently high quality were not available for separation of the reflections observed at close positions owing to the long c axis (56.910(2) Å). One Me_3Si group was disordered over two positions in a ratio of 0.6:0.4, where the C atoms were refined isotropically. In **10**, the disordered C atoms around Si(1) and Si(2) both with occupancies of 0.5:0.5 were all refined isotropically.

Acknowledgment. We thank Mr. Kazumasa Oya for his experimental assistance. This work was supported by a Grant-in-Aid for Scientific Research on Priority Areas (No. 18065005, "Chemistry of Concerto Catalysis" to Y.M.) and a Grant-in-Aid for Scientific Research (B) (to H.S.) from the Ministry of Education, Culture, Sports, Science and Technology, Japan.

Supporting Information Available: Crystallographic data of **3a**·THF, **6**·0.8MeCN, **9a**, and **10** in CIF format. This material is available free of charge via the Internet at http://pubs.acs.org.

---

(27) *CrystalClear 1.3.5*; Rigaku Corporation: The Woodlands, TX, 1999−2003.

(28) *CrystalStructure 3.8.0*; Rigaku and Rigaku/MSC: The Woodlands, TX, 2000−2006.

(29) PATTY: Beurskens, P. T.: Admiraal, G.; Beurskens, G.; Bosman, W. P.; Garcia-Granda, S.; Gould, R. O.; Smits, J. M. M.; Smykall, C. *The DIRDIF program system, Technical Report of the Crystallography Laboratory*; University of Nijmegen: Nijmegen, The Netherlands, 1992.

(30) DIRDIF99: Beurskens, P. T.; Admiraal, G.; Beurskens, G.; Bosman, W. P.; de Gelder, R.; Israel, R.; Smits, J. M. M. *The DIRDIF-99 program system, Technical Report of the Crystallography Laboratory*; University of Nijmegen: Nijmegen, The Netherlands, 1999.